Decreasing luminescence lifetime of evaporating phosphorescent droplets

Please check the document version of this publication:

• A submitted manuscript is the version of the article upon submission and before peer-review. There can be important differences between the submitted version and the official published version of record. People interested in the research are advised to contact the author for the final version of the publication, or visit the DOI to the publisher's website.
• The final author version and the galley proof are versions of the publication after peer review.
• The final published version features the final layout of the paper including the volume, issue and page numbers.

[Link to publication](#)

Decreasing luminescence lifetime of evaporating phosphorescent droplets

D. D. van der Voort, N. J. Dam, A. M. Sweep, R. P. J. Kunnen, G. J. F. van Heijst, H. J. H. Clercx, and W. van de Water

Decreasing luminescence lifetime of evaporating phosphorescent droplets

D. D. van der Voort,[1,a)] N. J. Dam,[2] A. M. Sweep,[2] R. P. J. Kunnen,[1] G. J. F. van Heijst,[1] H. J. H. Clercx,[1] and W. van de Water[1]

[1]J. M. Burgers Center for Fluid Dynamics and Turbulence and Vortex Dynamics, Applied Physics Department, Eindhoven University of Technology, 5612 AZ Eindhoven, The Netherlands
[2]Mechanical Engineering Department, Eindhoven University of Technology, 5612 AZ Eindhoven, The Netherlands

Laser-induced phosphorescence has been used extensively to study spray dynamics. It is important to understand the influence of droplet evaporation in the interpretation of such measurements, as it increases luminescence quenching. By suspending a single evaporating n-heptane droplet in an acoustic levitator, the properties of lanthanide-complex europium-thenoyltrifluoroacetone-trioctylphosphine oxide (Eu-TTA-TOPO) phosphorescence are determined through high-speed imaging. A decrease was found in the measured phosphorescence decay coefficient ($780 \rightarrow 200\,\mu$s) with decreasing droplet volumes ($10^{-9} \rightarrow 10^{-11}$ m^3) corresponding to increasing concentrations ($10^{-4} \rightarrow 10^{-2}$ M). This decrease continues up to the point of shell-formation at supersaturated concentrations. The diminished luminescence is shown not to be attributable to triplet-triplet annihilation, quenching between excited triplet-state molecules. Instead, the pure exponential decays found in the measurements show that a non-phosphorescent quencher, such as free TTA/TOPO, can be attributable to this decay. The concentration dependence of the phosphorescence lifetime can therefore be used as a diagnostic of evaporation in sprays. *Published by AIP Publishing.* [http://dx.doi.org/10.1063/1.4971987]

Characterization of the high velocities and small scales of sprays in applications such as fuel spray combustion and spray drying benefits greatly from the use of the fast diagnostics enabled by high-power pulsed lasers, such as the laser-induced fluorescence (LIF) and laser-induced phosphorescence (LIP).[1,2] Both LIF and LIP are based on the absorption of laser energy by atoms and molecules and typically show a Stokes shift of the emission wavelength. LIP can be used for relatively long-lifetime (ms) applications, such as flow tracking.[3,4] In particular, single-phase phosphorescent tracers (such as lanthanide-based organic complexes) can be used to exclusively visualize and track the liquid content in a spray.[5] The phosphorescent compounds can be characterized by their lifetime, and the concentration of excited molecules can at any time directly be related to the liquid content. However, in previous work it was found that the luminescence lifetime itself may become time-dependent, likely as a result of evaporation[6] (see Figure 1). Especially when the timescale of the evaporation becomes similar to the timescale of the flow, the role of non-radiative decay processes (quenching) due to molecular interactions become essential for quantitative interpretations.

Transfer of energy to a different molecule, such as oxygen, is a common cause of quenching. Another likely quenching process is triplet-triplet annihilation,[7–9] where triplet or higher spin states of the phosphorescent molecule decay to a singlet state through spin catalysis.[10] These processes all depend on molecular concentrations, and their effects on decay rates and emission intensity may provide a quantitative diagnostic of evaporation. In the past, the effect of evaporation on droplet phosphorescence has been investigated using droplet streams.[11,12] However, this severely

limits the visualization time. The long time-scales involved in evaporation at low (293 K) temperatures require a suspension of a droplet in air, which can be achieved using acoustic levitation.[13] Omrane *et al.*[14] investigated the evaporation of suspended droplets, where the temperature sensitivity of Eu-La$_2$O$_2$S phosphor was used to determine the droplet temperatures, a technique often used in phosphor thermometry. However, the influence of strong evaporation on the phosphorescence lifetime and emission intensity is still unknown. In this work, the phosphorescence of evaporating droplets is investigated by levitating the droplets in air through the use of an acoustic standing wave. In this non-reactive environment with good optical accessibility, the phosphorescence decay and its quenching mechanism are investigated as a function of the droplet volume/concentration. To investigate the evaporation with the interface chemistry similar to droplet-laden flows, the liquid needs to be completely surrounded by a gas. An acoustic levitator, based on the acoustic streaming effect, can be used to suspend a droplet in air.[15] By generating a standing ultrasound wave (see Figure 2), the weight of a droplet in a nodal point is offset by the pressure
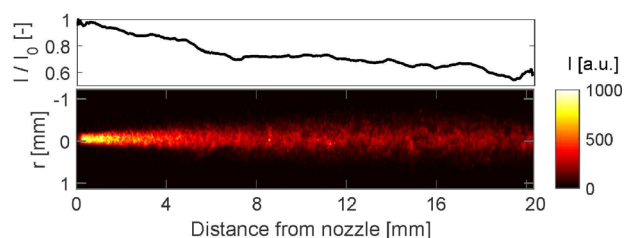

FIG. 1. A luminescent spray, excited inside the nozzle. All liquid in this spray was excited at the same instant, and the decrease in radially integrated luminescence over distance is more than changes in morphology can account for Ref. 6, and is likely due to evaporation.
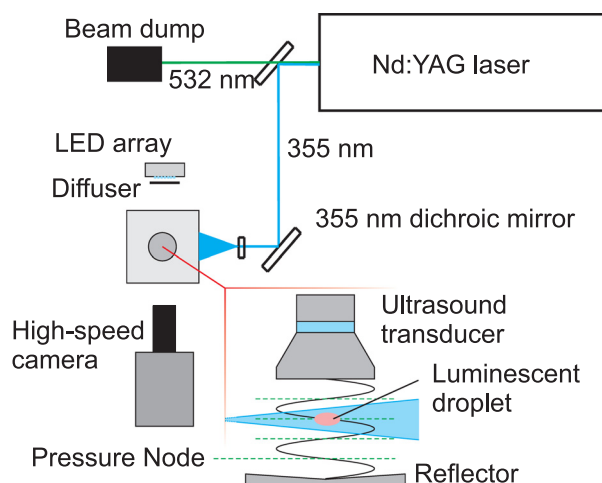
a)d.d.v.d.voort@tue.nl

FIG. 2. Schematic of the experimental setup. A droplet is suspended in one of the nodes of a standing wave between an ultrasound transducer and a reflector. It is excited with a UV laser, and the luminescence emitted by the droplet is captured by a high-speed camera.

FIG. 3. An acoustically suspended 1.5 mm droplet less than 10 s after insertion, 5 μs after excitation (a), and illuminated by a field of diffuse LEDs (b). The direction of laser light incidence is indicated with the blue arrows. Large droplets are deformed into oblate spheroids by the acoustic field; they become spherical at diameters below approximately 200 μm.

force exerted by the standing wave. The size of the droplet is therefore limited by its proportion to the ultrasound wavelength λ_s, with a maximum at approximately $\lambda_s/2$, while the lower limit (∼150 μm diameter) is determined by the stability of the droplet. The levitator in Figure 2 consists of a 40 kHz Langevin ultrasound transducer (Steiner & Martins Inc.), with the frequency, a trade-off between the power and range of droplet sizes, powered by a Citronic PLX2000 amplifier (AVSL group, UK). The transducer creates a standing wave in combination with a shallow cone reflector with a center depth of 5 mm and a radius of 5 cm (i.e., a 2.9° angle), to increase the lateral positional stability of the droplet within the acoustic field (supplementary material).

The third harmonic of a pulsed Nd:YAG laser is formed into a wide sheet which envelops the suspended droplet. Upon insertion into the levitator, the droplets nominally contain a 10^{-4} M concentration of europium-thenoyltrifluor-oacetone-trioctylphosphine oxide (Eu-TTA-TOPO), in a heptane solution (99% Reagentplus, Sigma-Aldrich). The Eu-TTA-TOPO is a phosphorescent lanthanide supramolecule with a phosphorescence lifetime in the order of milliseconds at a dominant wavelength of $\lambda \approx 614$ nm. It is one of the lanthanide complexes useful for flow tracking and evaporation investigations.[5,6,16,17] The UV light induces phosphorescence, and the emitted light is measured with a Photron SA-X2 camera and Nikon AF micro 70–180 mm lens to obtain a framerate of 15 kHz and resolution of 14.7 μm/pixel, respectively (see Figure 3(a)). The recordings start 5 μs after the excitation, to ensure that all fluorescence has died out. Figure 3(a) shows the droplet phosphorescence after excitation, exhibiting a small pattern caused by the focusing of the incident laser light by the droplet.[18] The phosphorescence measurements are repeated at a frequency of 1–2 Hz until the droplet disappears from the trap. The size of the droplet is determined through the Canny edge detection, which requires the droplet to be in focus. Therefore diffuse-backlight illumination is used (see Figure 3(b)) before the start of the phosphorescence measurement to monitor the position and focus of the droplet, immediately after its insertion
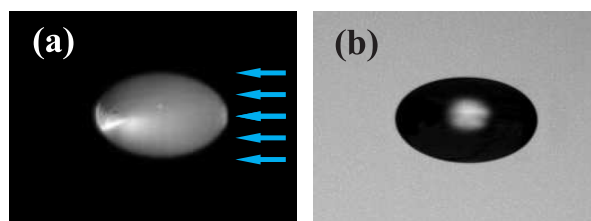
with a 32 gauge needle. Figure 4 shows that the rate of evaporation for the heptane droplets, both with and without added phosphorescent complex, follows the well-established[19] R-squared law $R^2(t_e) = R^2(0) - \beta t_e$, with the evaporation rate $\beta = 2DM\Delta P/\rho_l\mathcal{R}T$, where $D = 6.5 \times 10^{-6}$ m^{2}s^{-1} is the diffusion coefficient, $M = 100.2$ g/mol the molecular weight of heptane, $T = 293$ K the temperature, $\mathcal{R}$ the gas constant, ρ_l the density of the evaporating fluid, t_e the evaporation time, and ΔP the vapour pressure difference between the surface of the droplet and the surrounding air. Assuming ΔP is equal to the saturation vapour pressure of heptane, the theoretical evaporation rate is $\beta_{th} \approx 4 \times 10^{-9}$ m^2 s^{-1}, which does not significantly differ from the experimentally found value of $\beta_{exp} = 3.9 \times 10^{-9}$ m^2 s^{-1} for a pure heptane droplet. The small difference in evaporation rate when the phosphorescent compound is added, $\beta_{exp,ph} = 3.5 \times 10^{-9}$ m^2 s^{-1}, can be explained by the slowdown in evaporation caused by molecules accumulating at the interface, yet remaining porous enough to hardly affect the evaporation.[20]

Next, we will discuss the time dependence and emission intensity of the phosphorescence. Figure 5 shows that at large droplet sizes, the total luminescence intensity $I(0)$ decreases with the (projected) surface area R^2, and for small

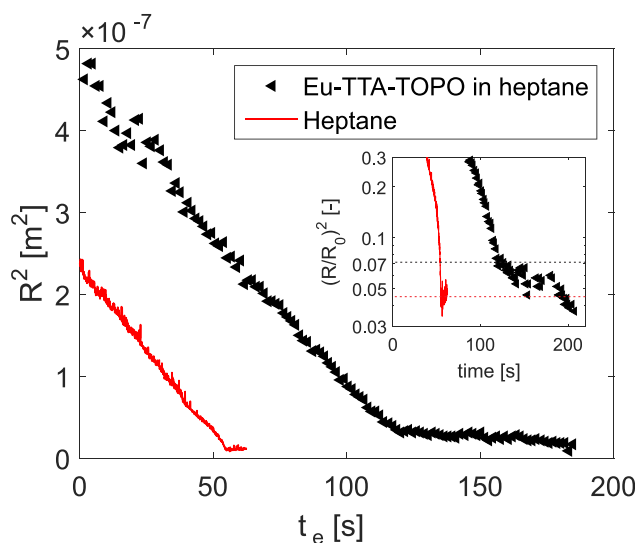FIG. 4. The change of the droplet radius over time for a pure solvent (red) and with added phosphorescent compound (triangles). The trend follows the r-squared law, indicating a diffusion controlled evaporation, with a strong change in evaporation rate at droplet radii under 200 μm. The inset figure shows the measurement normalized to the initial droplet radius R(0), with the dotted lines indicating the point of transition.
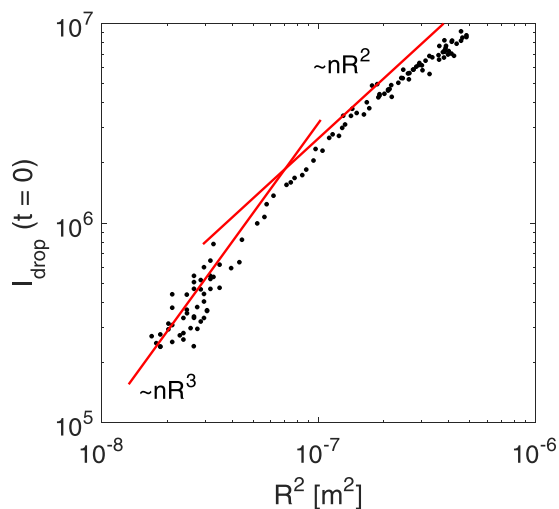
FIG. 5. The measured luminescence intensity, immediately after excitation, versus the surface area of the droplet. The lines indicate linear relations with the laser illuminated surface area of the droplet ($\propto nR^2$) for large droplets, and with the droplet volume ($\propto nR^3$) for small droplets.

droplets with R^3. While the intensity decreases for large droplets with the laser-illuminated area, indicating that the excitation is not saturated, for small droplets (and thus large concentrations), the excitation efficiency decreases inversely proportional to the concentration. As the evaporation timescale t_e [$O(s)$] is much longer than the phosphorescent lifetime [$O(ms)$], each measurement of the phosphorescence intensity over time $I(t)$ is at a single value of the droplet radius. For each measurement, $I(t)$ is fitted to single exponential decay ($I = I_0 \times e^{-t/\tau}$) to determine the phosphorescence decay time τ (see Figure 6).

We assume that the initial concentration is 10^{-4} M, neglecting evaporation occurring between droplet insertion and the start of the measurement. The change in volume over time can then be rephrased as a change in concentration, as in Figure 7. This shows that as the concentration increases,
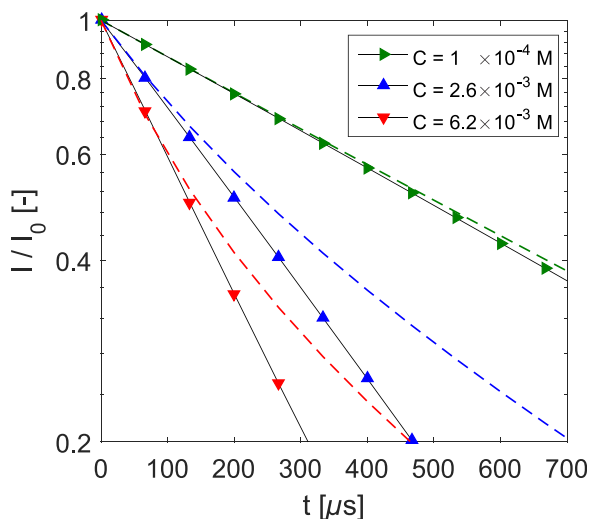

FIG. 6. The droplet luminescence intensity I (normalized by the intensity I_0 at $t = 0$) as a function of time after excitation, with experimental data in solid lines for different concentrations (i.e., droplet diameters), and the results for the triplet-triplet annihilation model in dashed lines for $k_{TT} = 1.6 \times 10^6 \, s^{-1}$. In contrast to the annihilation model, the experiments show only a pure exponential decay.
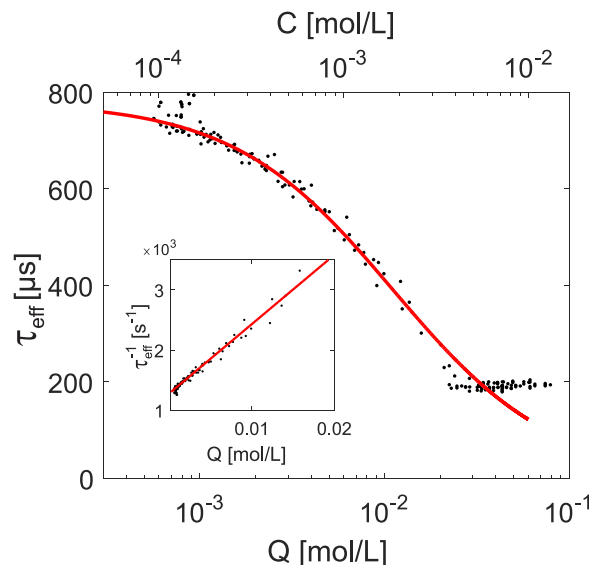

FIG. 7. The change in the phosphorescence decay coefficient τ_{eff} as a function of the (hypothesized) quencher and Eu-TTA-TOPO concentration. The red line shows the non-phosphorescent quencher model for a rate constant of $k_Q = 1.2 \times 10^5 \, s^{-1}$.

the phosphorescence lifetime diminishes. An increase in temperature due to the UV excitation is a possible explanation, but the low fluence of the excitation light, the temperature insensitivity of τ around room temperature, and measurements with a thermal camera (Flir S40), exclude this possibility. A more likely candidate to explain the observed decrease is quenching by triplet-triplet annihilation, where interaction between triplet state molecules results in a radiationless decay to a singlet or ground state,[9] that is, $^*P^3 + ^*P^3 \rightarrow ^*P^1 + P$ and $^*P^3 + ^*P^3 \rightarrow ^*P^3 + P$, with $^*P^3$ the triplet excited state, $^*P^1$ the singlet excited state, and P the singlet ground state of the phosphorescent tracer molecule. In the case of triplet-triplet annihilation, the concentration C of the excited triplet states $^*P^3$ satisfies

$$\frac{dC}{dt} = -\frac{1}{\tau}C - \frac{1}{2}k_{TT}C^2, \tag{1}$$

with $\frac{1}{2}k_{TT}$ the rate constant of the annihilation process, with a 1/2 prefactor as a new triplet molecule is generated for each annihilation event. Assuming that the luminescence intensity is proportional to C, the solution of (1) leads to

$$I(t) = \frac{I(0)}{\left(\frac{1}{2}k_{TT}C(t_e)\tau + 1\right)e^{\frac{t}{\tau}} - \frac{1}{2}k_{TT}C(t_e)\tau}, \tag{2}$$

with t_e the timescale of the evaporation, t the timescale of the phosphorescence, and $I(0)$ the luminescence intensity immediately after excitation. With decreasing droplet diameter d, $C(t_e) \sim d^{-3}$ increases and the decay of intensity should become increasingly non-exponential. The result of our experiment is a fan of decay curves for varying concentration $C(t_e) = C_s(d_s/d(t_e))^3$, where C_s is the stock concentration, d_s the diameter of the initial droplet size before evaporation, and $d(t_e)$ the droplet diameter at each lifetime measurement. If the decay of the phosphorescence lifetime would be due to triplet-triplet annihilation, two parameters, viz., k_{TT} and τ,

should suffice to reproduce all curves. Our best fit in Figure 6 shows that this is not the case. This is corroborated by the observation that all decay curves are purely exponential.

We hypothesize that the triplet molecules are quenched by a non-luminescing molecule that is used in the preparation of the phosphorescing complex, and which does not evaporate. Let us call Q the concentration of this agent where, analogous to C, $Q(t_e) = Q_s(d_s/d(t_e))^3$, with Q_s the quencher concentration before evaporation. The exponential decay of the luminescence intensity then simply follows from

$$\frac{dC}{dt} = -\frac{C}{\tau_{\text{eff}}}, \qquad (3)$$

with $1/\tau_{\text{eff}} = 1/\tau_0 + k_Q Q$, where τ_0 is the decay coefficient at zero concentration of Q and k_Q the rate constant of the triplet to singlet decay. In Figure 7, we plot $1/\tau_{\text{eff}}$ versus Q, assuming that $Q_s \approx 6 \times 10^{-4}$ (approximately equal to the concentration of free TTA/TOPO compounds), and demonstrate that this relation holds very well until $Q \approx 2 \times 10^{-2}$ M. Thus we prove that the decay time is a precise probe of the concentration of the phosphorescent complex. Obviously, the numerical values of Q and k_Q will vary with tracer concentration and composition. (The phosphorescent liquid is a mixture of various compounds, and we cannot tell which of the components, if any in particular, plays the role of Q.)

At approximately $Q = 2 \times 10^{-2}$ M, the decay time no longer decreases with decreasing droplet size. The sudden kink in $\tau_{\text{eff}}(Q)$ corresponds to that of Figure 4, where the decrease of $R^2(t_e)$ abruptly slows down, but is still approximately linear. We hypothesize that at this point solute molecules sit in a concentric shell bounded by the liquid-air interface, such that the thickness of the shell increases while evaporation continues, but the distance between molecules remains (nearly) constant. This is illustrated in Figure 8, which shows an increased luminescence at the boundary of the droplet for increasing concentrations, also observed by Omrane *et al.* for non-soluble phosphor compounds.[14]
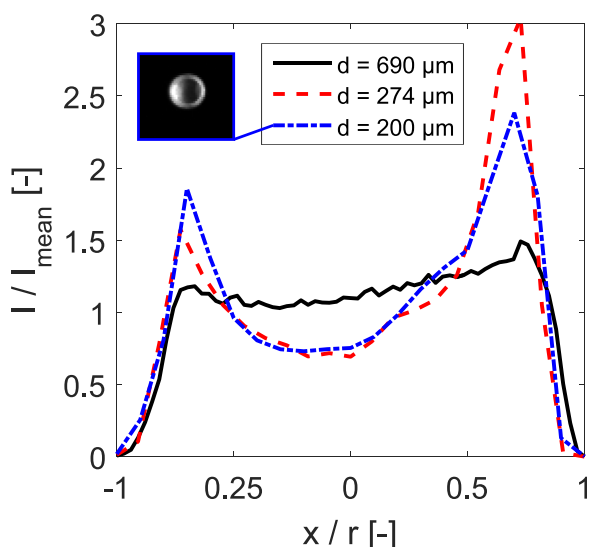

FIG. 9. Shell formation around an evaporating droplet, resulting in highly asymmetric phosphorescence intensity profiles.

Shell formation has similarly been found in evaporation of colloidal droplets.[20–22] When the evaporative flux of the solvent is stronger than the diffusion of particles or heavy molecules inside the fluid, a shell will form around the droplet.[21,23] This is furthermore corroborated by the asymmetric intensity profile at very small droplet size, indicative of buckling/broken shell formations; an example shown in Figure 9. In case of a porous shell, the droplet radius will still decrease as $R^2(t) = R^2(0) - \beta t$, but now β is determined by the diffusion of the heptane solvent through the shell. From the change of slope in Figure 4, we estimate that the associated diffusion coefficient is a factor of 10 smaller than that of diffusion through air. In this configuration, the distance between the molecules in the shell does not change, and the lifetime stabilizes. A similar kink is observed in the evaporation of pure heptane droplets. This occurs at the purity limit of the solvent, which occurs when 0.8% of the original volume remains (as shown in the insert of Figure 5), while the kink for the phosphorescent solution occurs at 1.9% of the remaining volume.

Non-uniform light emission by excited droplets has previously been found in fluorescence studies,[18,24] where light refraction caused an increasing luminescence due to focusing of the laser, and Lambert-Beer absorption causes an increasing edge luminescence at the illuminated surface. However, both of these effects are only applicable in the direction of the incoming light, which does not explain the increased edge luminescence perpendicular to (and independent of) the incoming laser direction.

In summary, we find that the lifetime of a phosphorescent agent is a sensitive probe of its concentration in evaporating droplets. When the concentration is reached where shell formation occurs, the lifetime no longer decreases. The change of lifetime, luminosity, and the occurrence of shell formation determines the range of droplet sizes that can be tracked using phosphorescent flow diagnostics. With a known concentration dependence, the local decay rate of the phosphorescence can be used as a measure of evaporation.

See supplementary material for a DBI recording of an evaporating suspended droplet, visualizing the stability of the droplet inside the acoustic levitator as a function of size.

FIG. 8. The centerline horizontal radial intensity profiles over the droplet radius for different droplet sizes.

[1] J. Dec, SAE Technical Paper No. 970873 (1997).
[2] M. Linne, Prog. Energy Combust. Sci. **39**, 403 (2013).

[3]S. Krüger and G. Grünefeld, Appl. Phys. B **71**, 611 (2000).

[4]S. Wissel, T. Hoffmann, P. Hottenbach, H. Koss, C. Pauls, and G. Grünefeld, SAE International No. 2008-01-0944 (2008).

[5]D. van der Voort, B. de Ruijter, W. van de Water, N. Dam, H. Clercx, and G. van Heijst, Atomization Sprays **26**, 219 (2016).

[6]D. van der Voort, N. Maes, T. Lamberts, W. van de Water, R. Kunnen, H. Clercx, G. van Heijst, and N. Dam, Rev. Sci. Instrum. **87**, 033702 (2016).

[7]W. Staroske, M. Pfeiffer, K. Leo, and M. Hoffmann, Phys. Rev. Lett. **98**, 197402 (2007).

[8]J. Ribierre, A. Ruseckas, K. Knights, S. Staton, N. Cumpstey, P. Burn, and I. Samuel, Phys. Rev. Lett. **100**, 017402 (2008).

[9]M. A. Baldo, C. Adachi, and S. Forrest, Phys. Rev. B **62**, 10967 (2000).

[10]A. Buchachenko and V. Berdinsky, Chem. Rev. **102**, 603 (2002).

[11]A. Charogiannis and F. Beyrau, Exp. Fluids **54**, 1518 (2013).

[12]A. Omrane, G. Juhlin, F. Ossler, and M. Alden, Appl. Opt. **43**, 3523 (2004).

[13]A. Yarin, G. Brenn, O. Kastner, D. Rensink, and C. Tropea, J. Fluid Mech. **399**, 151 (1999).

[14]A. Omrane, S. Santesson, M. Alden, and S. Nilsson, Lab Chip **4**, 287 (2004).

[15]A. Yarin, M. Pfaffenlehner, and C. Tropea, J. Fluid Mech. **356**, 65 (1998).

[16]N. Arnaud and J. Georges, Spectrochim. Acta, Part A **59**, 1829 (2003).

[17]T. Brands, P. Hottenbach, H. Koß, G. Grünefeld, S. Pischinger, and P. Adomeit, J. Phys. Sci. Appl. **3**, 279 (2013).

[18]B. Frackowiak and C. Tropea, Appl. Opt. **49**, 2363 (2010).

[19]W. Niven, *The Scientific Papers of James Clerk Maxwell*, 1st ed. (Dover Publications, 1890).

[20]D. Charlesworth and W. Marshall, Jr., Am. Inst. Chem. Eng. **6**, 9 (1960).

[21]C. Sadek, P. Schuck, Y. Fallourd, N. Pradeau, C. L. Floch-Fouere, and R. Jeantet, Dairy Sci. Technol. **95**, 771 (2015).

[22]A. Marin, H. Gelderblom, A. Susarrey-Arce, A. van Houselt, L. Lefferts, J. Gardeniers, D. Lohse, and J. Snoeijer, Proc. Natl. Acad. Sci. USA **109**, 16455 (2012).

[23]N. Tsapis, E. Dufresne, S. Sinha, C. Riera, J. Hutchinson, L. Mahadevan, and D. Weitz, Phys. Rev. Lett. **94**, 018302 (2005).

[24]R. Domann and Y. Hardalupas, Appl. Opt. **40**, 3586 (2001).